Flame-retardant action of red phosphorus/magnesium oxide and red phosphorus/iron oxide compositions in recycled PET

F. Laoutid, Laurent Ferry, J. Lopez-Cuesta, A. Crespy

Flame-retardant action of red phosphorus/magnesium oxide and red phosphorus/iron oxide compositions in recycled PET

F. Laoutid[1], L. Ferry[1], J. M. Lopez-Cuesta[1,*,†] and A. Crespy[2]

[1] *Centre des Matériaux de Grande Diffusion (C.M.G.D), Ecole Des Mines d'Alés 6, Avenue de Claviéres, 30319 Alés Cedex, France*
[2] *Matériaux á finalités spécifiques, Université de Toulon et du Var, BAT. 118, BP 132, 83957 La Garde Cedex, France*

SUMMARY

Red phosphorus was combined with metallic oxides Fe_2O_3 and MgO to improve the fire properties of recycled PET. Both Fe_2O_3 and MgO act as co-synergist agents at a total loading of 5 wt%. The analysis by diffraction *X* of the char formed during combustion shows that transformation of Fe_2O_3 to Fe_3O_4 occurs. Fe_2O_3 favours the oxidation and improves the effectiveness of red phosphorus. It is suggested that MgO interacts with acidic end groups of PET and forms a thermal stable residue. The thermal decomposition of recycled PET containing red phosphorus combined with Fe and Mg oxides was studied by thermal analysis and leads to an increase in char formation. While the incorporation of Fe_2O_3 in this ternary blend maintains the mechanical properties of PET, the reactivity of MgO leads to a brittle material. The use of reinforcements (talc and glass fibres) to mechanically stabilize the char formed during combustion of ternary blend with Fe_2O_3 entails a further decrease in heat release rate, nevertheless impact resistance of the material decreases dramatically.

KEY WORDS: PET recycling; flame retardant; red phosphorus; iron oxide; magnesium oxide

0. INTRODUCTION

The applications of regenerated PET issued from recollection of beverage bottles concern mainly the elaboration of fabrics due to the reprocessing difficulties of this reclaimed material. A decrease in molecular weight for recycled PET in comparison with virgin PET is usually noticed [1]. This phenomenon is ascribed to chain breakages due to the presence of traces of water and acidic impurities. Consequently, the reuse of recycled PET as a structural material is limited. Moreover, the need to confer new properties to recycled PET in order to obtain engineered plastics is also dependent on the improvement of thermal stability and fire performances.

After preparing a PET with controlled mechanical properties (by drying and elimination of impurities) from a commercial recycled PET, the objective of this work was to improve its

*Correspondence to: Jose-Marie Lopez-Cuesta, Centre des Materiaux de Grande Diffusion (C.M.G.D), Ecole des Mines d'Ales, 6, Avenue de Clavieres, 30319 Ales Cedex, France.
† E-mail: Jose-Marie.Lopez-Cuesta@ema.fr

resistance to flammability using new kind of flame-retardant systems based on synergistic effects. Red phosphorus (noted red P) was chosen as a component of these flame-retardant systems because of its strong flame-retardant (FR) action at low percentages in oxygen-containing polymers. The possibility of working safe from phosphine emission thanks to the use of masterbatch was also considered. We also focused on the research of co-synergists agents of red P as well as on the understanding of the mechanisms of thermal degradation and flammability of recycled PET containing such flame-retardant systems.

In a previous paper [2], it was noticed that the improvement of the fire performances of PET tends to level off from a 5% weight and then to decrease when the red P percentage is increased. This evolution could be explained by the influence of the oxidation of red P which could increase the volatile combustibles production and counterbalance its flame-retardant effect. It has also been shown that the use of Al_2O_3 in partial substitution of red P could increase limiting oxygen index (LOI) values and decrease the rate of heat release (RHR) for cone calorimeter tests. The influence of high surface specific area was highlighted on synergistic performance of alumina obtained from alumina trihydrate after calcination.

A previous study on the combination of red P with some metallic oxides (Al_2O_3 and MgO) was made by Yeh *et al*. [3]. Nevertheless, the mechanism of action of these oxides was not fully explained. The role of their morphology was not studied and only LOI values were presented to characterize fire resistance. In this paper, we tried to assess and to investigate the role of MgO as red P synergist. Moreover, several metallic oxides were tested as potential synergist agents, particularly iron oxide, which was mentioned as a synergistic agent with red P in PA-6 by Levchik *et al*. [4] and also pointed out by Weil and Patel [5,6]. Recently, Laachachi *et al*. [7] have shown that Fe_2O_3 could also increase the thermal stability of PMMA by reducing the chain mobility as proved by the evolution of Tg. Owing to its significant influence, results concerning Fe_2O_3 are also presented.

Finally, in order to improve the stability of char formed after combustion of PET containing red P combined with metallic oxides, reinforcing components (talc and glass fibres) were also added.

1. EXPERIMENTAL PART

1.1. Materials

The PET flakes were supplied by the Valorplast Company, which is in charge of the collection of post-use waste packaging in France.

The masterbatch Red P/PA-6 was provided by Italmatch. The composition of the masterbatch was 50% w/w of each component. Magnesium oxide was obtained by calcination of magnesium hydroxide Magnifin H 10 (Martinswerk). The median particle size of the raw material is 1 μm with a BET surface area of 9.5–11 m^2/g. Iron oxide (hematite) was supplied by Panreac (median particle size is 2.5 μm, specific surface area is 8.2 m^2/g).

1.2. Techniques

1.2.1. Compositions, blending and processing. Red P was incorporated in recycled PET up to a value of 5% phosphorus in weight. Metal oxides were incorporated in partial substitution of red P, the total loading was kept constant at 5 wt%.

Masterbatches of metal oxides with PET were made by twin-screw extrusion (Clextral BC 21, France) and blended with masterbatch red P/PA and PET flakes for injection moulding (Sandretto, France). The processing temperature was 260–280°C depending on the compositions.

Glass fibres and talc were incorporated at 6% w/w percentage in addition to the flame-retardant system (red P alone or with metal oxides). A talc masterbatch was elaborated using twin-screw extrusion and a commercial masterbatch of glass fibres was used. Reinforced glass fibres, talc and red P masterbatches were also blended with PET flakes prior to injection-moulding procedure.

The specimens elaborated were dumb-bell according to ISO 527-2 type 1A specifications and used for mechanical testing, $100 \times 100 \times 4$ mm sheets were used for flammability tests.

1.2.2. Physical and chemical characterizations

1.2.2.1. Thermal degradation and flammability. Thermal analysis and specific flammability experiments were carried out to characterize the thermal behaviour of PET. Thermal degradation studies in air and argon were performed using a differential thermogravimetric and thermal analyser (Setaram TGDTA92). The temperature profile used was 5°C/min from 25 to 700°C.

Flammability tests (LOI (ISO 4589) and 'epiradiateur test' (AFNOR NF P 92-505)) were also used. In this last test, a $70 \times 70 \times 4$ mm sheet is placed on a metallic grid below a 500 W radiator, the radiator is removed and replaced, respectively, after each ignition and extinguishing. The first time of ignition and the mean and maximal values of combustion times are determined. At least four specimens were tested for each composition.

The thermal behaviour was also tested by a cone calorimeter device (Fire Testing Technology). A $100 \times 100 \times 4$ mm sheet is exposed to a radiant cone (50 kW/m^2). The RHR can be calculated as a function of the oxygen consumption linked to the combustion of the specimen using an oxygen analyser.

1.2.2.2. Mechanical characterizations. Maximal tensile strength of dumb-bells was measured according to the ISO 178 standard and using an Adamel Lhomargy universal testing machine. Unnotched Charpy impact strength was determined using a Zwick apparatus according to ISO 179 standard.

1.2.2.3. Spectroscopic and microscopic characterizations. Combustion char residues were observed and studied using a SEM JEOL 35CF coupled with EDX. Crystalline mineral structures were identified by means of a Philips X-ray diffractometer. The chemical structure of the residue was also studied by FTIR spectroscopy (Bruker IFS 66).

2. RESULTS AND DISCUSSION

2.1. Incorporation of red P in recycled PET

The study of thermal decomposition (Figure 1) by TGA of recycled PET both in air and argon show a two-step decomposition. The first one correspond to the main decomposition (370–430°C) while the second one is due to the decomposition of a char residue more stable in argon

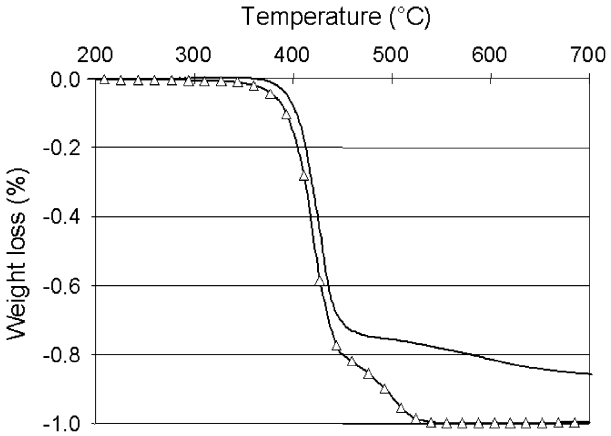

Figure 1. TGA curves (5°C/min) of PET in air and argon. (Δ) PET in air, (—) PET in argon.

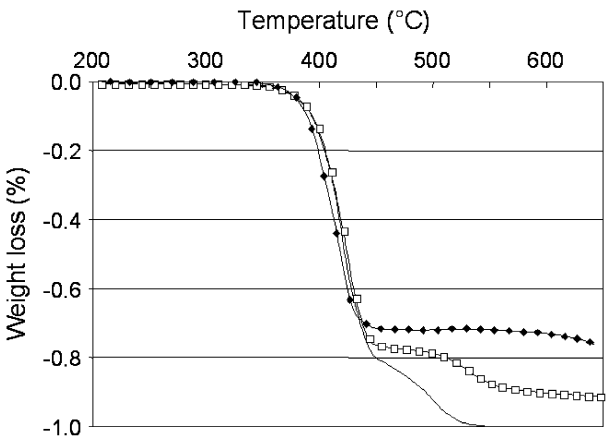

Figure 2. TGA curves of filled and unfilled PET in air (5°C/min). (—) PET, (□) 3% red P, (◆) 5% red P.

than in the air. At 3 and 5%, red P tends to promote the formation of a charred residue which is stable up to 650°C in air atmosphere (Figure 2). As shown by several authors concerning the action of red P on PET degradation [8,9], one can also consider that condensed phase mechanisms are predominant. The presence of oxygen in PET contributes to the formation of a phosphorus anhydride with increasing temperature, leading to phosphoric acid and then phosphoric polyacids causing a dehydration of PET and char formation.

The incorporation of red P in recycled PET lead also to an increase in LOI values from an initial value of 23% without phosphorus to 35% for 5% red P (Figure 3). However, the incorporation of 5% red P reduced the impact resistance. This can be ascribed to the size of red P particles (around 10 μm) and the poor interfacial adhesion between red P particles, PA and PET matrix. Moreover, the cone calorimeter tests showed that the incorporation of red P leads to a decrease in the RHR peak, but higher values were obtained for 5% red P than in case of 3%

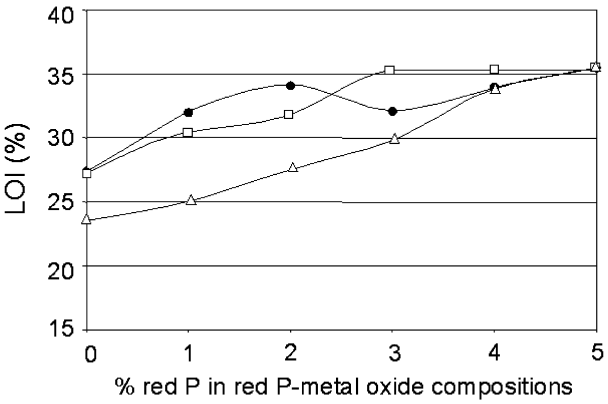

Figure 3. Limiting oxygen index (LOI) of PET as a function of the red P/metal oxide composition. (△) red P, (●) red P / Fe_2O_3, (□) red P/MgO. Total filler percentage equals 5%.

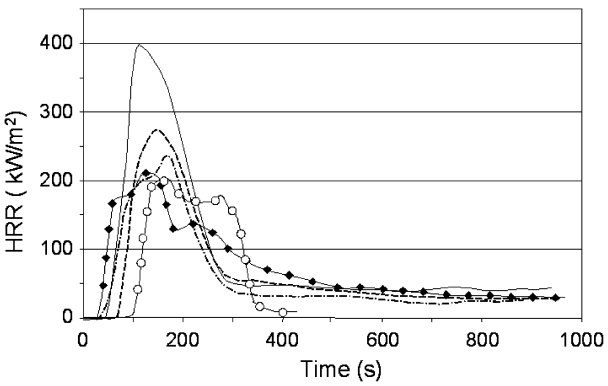

Figure 4. Heat release rate of filled and unfilled PET as a function of time. (—) PET, (–·–) 3% red P, (- - -) 5% red P, (◆) 3% red P + 2% MgO, (○) 3% red P + 2% Fe_2O_3.

red P (Figure 4). Consequently, the limitation in use of red P may suggest the use of co-synergists such as particular metallic oxides, able to limit these drawbacks.

2.2. Incorporation of MgO in combination with red P

Several substitution rates of red P by magnesium oxide were performed for a global percentage of 5% in PET. Figure 3 shows that synergism takes place for the LOI in the whole range of compositions. The first one provides the better value of LOI and the highest percentage of char residue measured at 500°C using TG analysis under air atmosphere. Figure 5 shows that additions of MgO to red P, particularly at 1 and 2%, accelerate the first degradation step of PET, but favour the formation of the char residue, by increasing its weight and thermal stability.

This residue is more stable with 3% red P + 2% MgO than that obtained with only 3% red P and begins to decompose from 550°C as observed also on DTA curves (Figure 6). Since TG

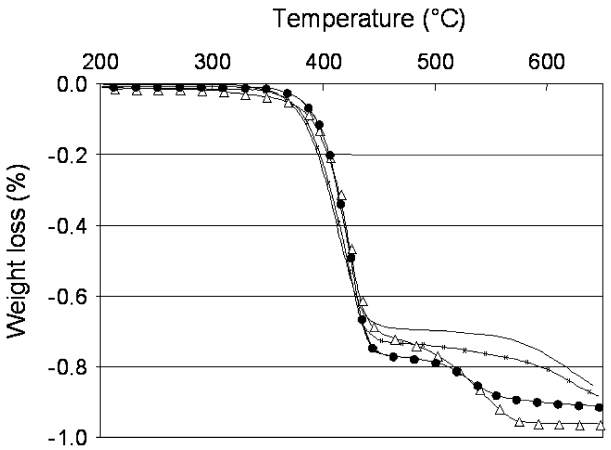

Figure 5. TGA curves in air (5°C/min) of filled PET with red P and MgO. (●) 3% red P, (—) 3% red P + 2% MgO, (Δ) 1% red P + 4% MgO, (x) 4% red P + 1% MgO.

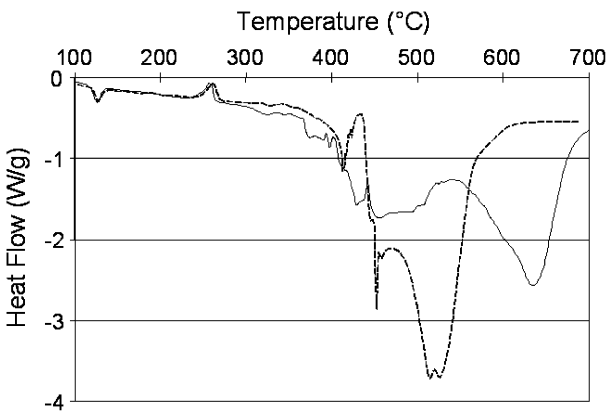

Figure 6. DTA curves of filled PET in air (5°C/min). (—) 3% red P, (- - -) 3 red P + 2% MgO.

decomposition curves in air and argon of this last composition are very similar up to 550°C (Figure 7), it appears that red P/MgO blends act mainly in the condensed phase like red P alone. The specific action of MgO corresponds to its ability to promote the creation of protective char layer. Epiradiateur test results (Table I) also show that the specific action of MgO improves the ability for the material to auto-extinguish, since the mean and maximal inflammation periods are identical for 3% red P + 2% MgO and 5% red P and lower than the value for only 3% red P. Moreover, the ignition time is significantly reduced in comparison to recycled PET and 3% red P composition due to an accelerated decomposition which could increase the quantity of volatile combustibles, leading to a more rapid ignition.

Consequently, this confirms that a synergistic action of red P and MgO occurs, causing an acceleration of the first step of degradation of PET and finally leading to a charred structure.

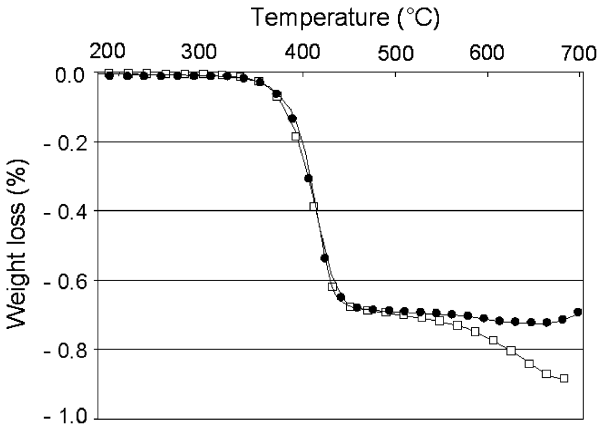

Figure 7. TGA curves (5°C/min) in air and argon of PET filled with 3% red P + 2% MgO. (□) in air, (●) in argon.

Table I. Epiradiateur test results of filled and unfilled PET.

Sample	Ignition time (s)	Mean inflammation period (s)	Maximal ignition period (s)
Recycled PET	188	20	23
3% red P	126	18	40
5% red P	113	8	15
3% red P + 2% MgO	105	8	14
3% red P + 2% Fe_2O_3	119	7	9

The synergistic action of MgO and red P can also be noticed in RHR curves. The RHR peak (Figure 4) is lower for 3% red P + 2% MgO than in the case of 5% red P.

This phenomenon may be caused by ionic interactions between MgO and the end acidic functions of PET (Figure 8). This formation of co-ordination chemical structures is well known in unsaturated polyesters and contributes to the formation of a tri-dimensional network and liberation of water. This tri-dimensional network could increase the amount of char formed during the combustion. In addition, the formation of water entails PET hydrolysis and increases its thermal decomposition.

The study of IR spectra of chars (Figure 9) obtained by combustion in a furnace at 500 and 600°C with the same temperature profile as in TG experiments is likely to indicate if its chemical structure was modified by the presence of MgO.

Chars corresponding to a burning unfilled PET (a), PET containing 3% red P at 500°C (b), PET containing 3% red P + 2% MgO at 500°C (c) and 600°C (d) were characterized.

We observed the presence of specific peaks (near 1600 and 700 cm^{-1}) on spectra (c and d) that are similar to those obtained for a PET char (a). This can be interpreted by considering that MgO also could favour the char formation of PET by stabilizing this structure.

In order to study the interactions between MgO and red P, the carbonaceous residues were studied by X-ray diffraction. Nevertheless, in spectrum corresponding to the residue after combustion at 500°C and at 5°C/min, the organic part of the residue prevented the analysis of a

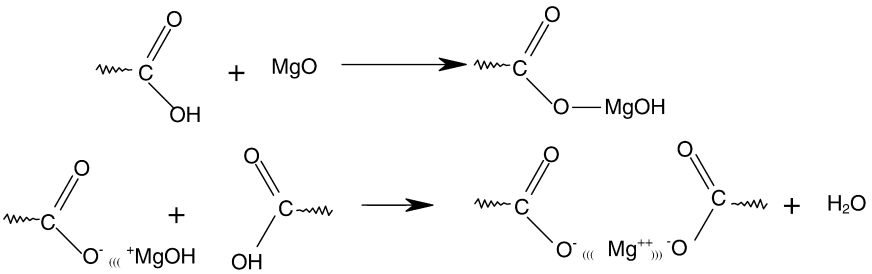

Figure 8. Ionic interactions between MgO and the acidic functions of PET.

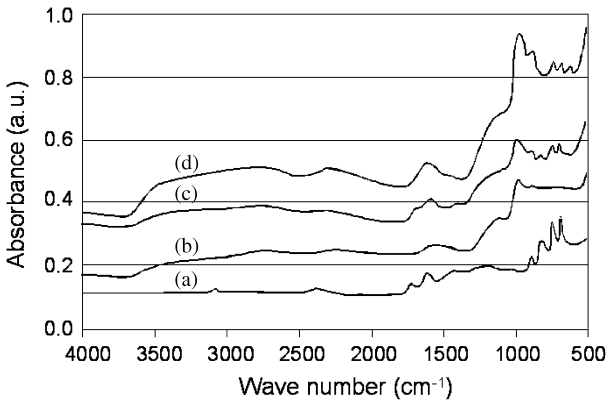

Figure 9. IRFT spectra of char of: (a) PET; (b) PET + 3% red P at 500°C; (c) PET + 3% red P + 2% MgO at 500°C; and (d) PET + 3% red P + 2% MgO at 600°C.

broad range of X-ray spectrum. Consequently, the analysis was performed on a sample maintained for 3 h at 600°C to eliminate this organic part corresponding to the PET residue.

The X-ray spectra (Figure 10) of the residue formed from PET containing 3% red P and PET containing 5% MgO showed no difference with the X-ray spectra of MgO. Nevertheless, two peaks corresponding to small quantities of magnesium phosphate appeared on the X-ray spectra.

Observations made using SEM and EDX on the chars corresponding to a burning PET containing 3% red P and 2% MgO at 500°C also showed the presence of dispersed particles of MgO on the surface of the char (Figure 11). At 600°C, the observations showed the presence of porous structures rich in phosphorus, oxygen and traces of magnesium oxide (Figure 12). However, due to the small dimensions of these structures, it was not possible to determine their chemical nature by nitration. Unlike Al_2O_3 [2], no significant chemical modification of MgO occurred. A part of this oxide contributes to the char formation but remains intact.

2.3. Incorporation of Fe_2O_3 in combination with red P

The evolution of LOI values of PET containing red P and Fe_2O_3 (Figure 3) shows a synergistic effect limited to low amounts of red P, particularly for the composition 2% red P + 3% Fe_2O_3.

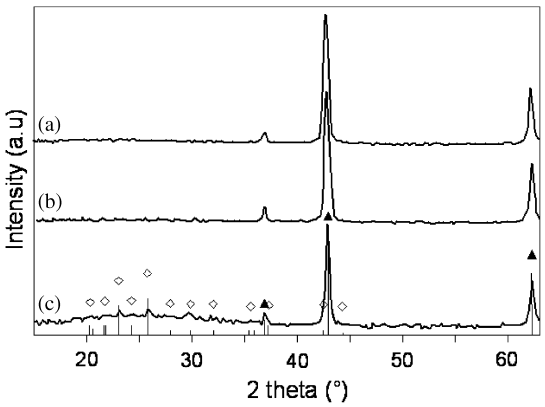

Figure 10. X-ray spectra of: (a) PET + 5% MgO; (b) MgO; and (c) PET +3% red P + 2% MgO. As reference, diffraction patterns of MgO (▲) and $Mg_3(PO_4)_2$ (◇) are represented.

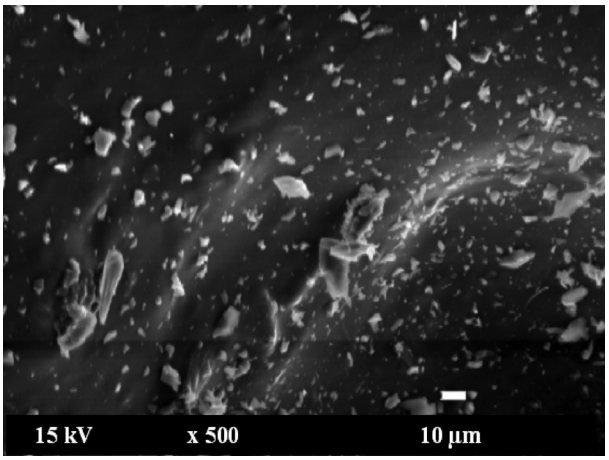

Figure 11. SEM micrograph of the residue formed at 500°C of PET + 3% red P + 2% MgO.

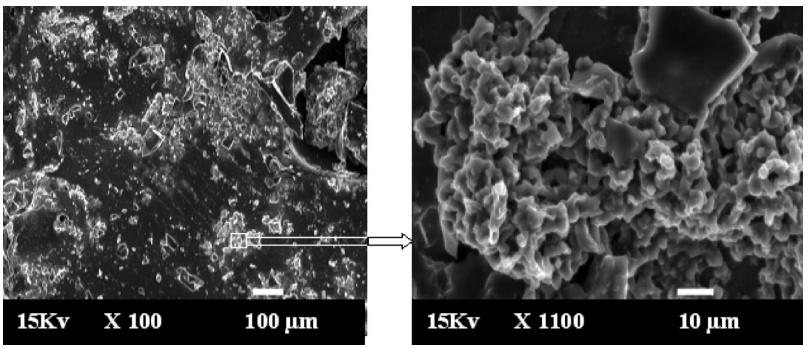

Figure 12. SEM micrographs (× 100, × 1100) of the residue formed at 600°C of PET +3% red P + 2% MgO.

Both components used together in recycled PET acts mainly by mechanisms acting in the condensed phase as red P alone, since TGA curves in air and argon are similar for the composition 3% red P + 2% Fe_2O_3 (Figure 13). For all these compositions, a stable char was formed at 500°C. Nevertheless, the thermal decomposition in air (Figure 14) of these compositions leads to the formation of different quantities of char. In fact, the residue formed was more important for 4% red P + 1% Fe_2O_3 than for 2% red P + 3% Fe_2O_3.

This suggests that iron oxide may act in different ways. To understand the specific contribution of Fe_2O_3, we studied the thermal decomposition in air of PET containing 5% of Fe_2O_3 and we measured the corresponding LOI value.

The thermal decomposition showed no formation of char residue but the LOI increased from 23.5 to 27.3%. This could be explained by a radical trapping action due to volatilized iron oxide particles during combustion.

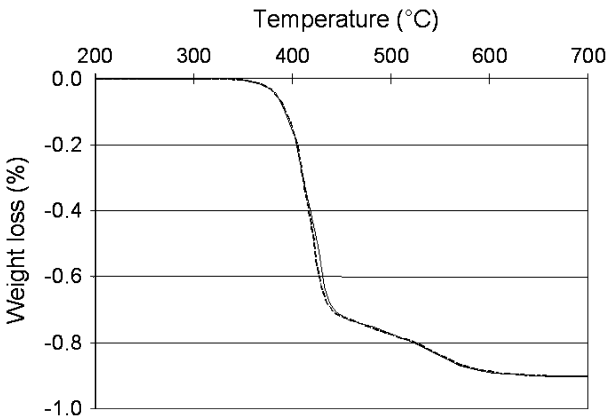

Figure 13. TGA curves (5°C/min) of PET filled with 3% red P + 2% Fe_2O_3 in air and argon. (—) in air, (- - -) in argon.

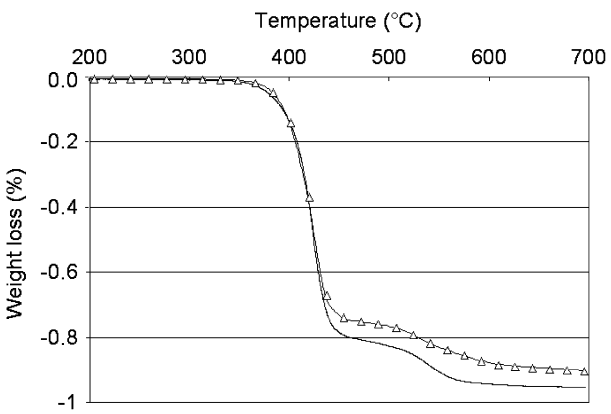

Figure 14. TGA curves in air (5°C/min) of filled PET. (Δ) 4% red P + 1% Fe_2O_3, (—) 2% red P + 3% Fe_2O_3.

Epiradiateur test results (Table I) also show that the specific action of Fe_2O_3 improves the ability for the material to auto-extinguish, by reducing both mean and maximal inflammation periods. The composition 3% red P + 2% Fe_2O_3 gives better results than compositions with red P alone. The ignition time value ranges between those of the compositions with 3 and 5% red P. This means that the incorporation of Fe_2O_3 with red P did not lead to an additional destabilization of PET in comparison with red P alone.

The synergistic action of Fe_2O_3 can also be observed in RHR curves (Figure 4). The substitution of 2% of red P by iron oxide leads to a modification of the curves. The RHR values decreases in comparison with the incorporation of 3 or 5% red P alone. The RHR peak is delayed and the RHR curve exhibits a plateau.

Char residues formed by calcination in a furnace at 500 and 600°C and corresponding to the composition 3% red P + 2% Fe_2O_3 were observed by SEM (Figure 15). The char seems cohesive at both temperatures, nevertheless some cracks appear at 600°C.

The X-ray spectra (Figure 16) of compositions containing only 5% Fe_2O_3 in PET show a conservation of Fe_2O_3 and no chemical interaction in condensed phase can be assumed. However, the X-ray spectra show that the combination of red P and Fe_2O_3 in PET leads to the

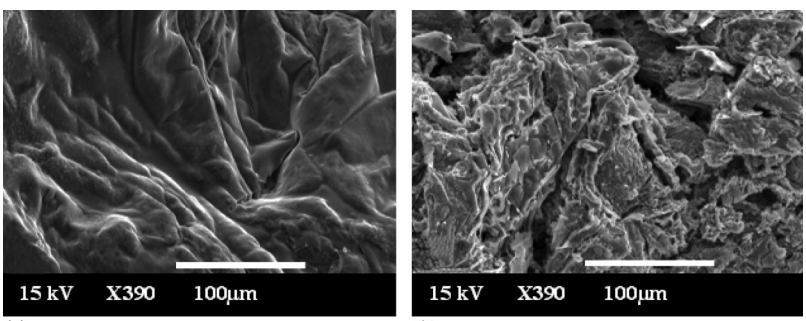

Figure 15. SEM micrographs of the residue of PET + 3% red P + 2% Fe_2O_3 formed at: (a) 500°C; and (b) 600°C.

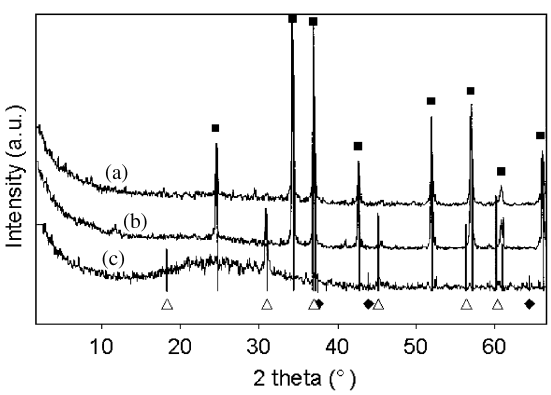

Figure 16. X-ray spectra of: (a) PET + 5% Fe_2O_3; (b) Fe_2O_3; and (c) PET + 3% red P + 2% Fe_2O_3. As reference, diffraction patterns of Fe_2O_3 (■), Fe_3O_4 (△) and FeO (♦) are represented.

formation of Fe_3O_4 and FeO. IR spectra (Figure 17) of the char residues obtained at 500 and 600°C also exhibit new peaks (corresponding to P═O bonds at 1200 cm^{-1} and P–O–P, P–C ($–C_6H_5$) bonds at 900 cm^{-1}) for the composition 3% red P + 2% Fe_2O_3. The interactions between red P and Fe_2O_3 differ significantly from these noticed with MgO (see above) and Al_2O_3 [2]. This means that Fe_2O_3 acts on the oxidation of red P. In consequence, iron is reduced in presence of phosphorus.

2.4. Mechanical properties of red P + oxides/PET compositions

It can be expected that the possible existing interactions between MgO and PET will significantly influence the mechanical properties of PET containing both MgO and red P. As a matter of fact, the corresponding specimens are brittle and the viscosity measured using a Rheometrics ARES viscosimeter could not be determined, due to the very low viscosity of the composition at molten state. The maximal tensile stress and elongation at break were also strongly reduced in comparison with PET containing only red P (Table II).

Conversely, the incorporation of iron oxide (composition 3% red P + 2% Fe_2O_3) did not cause dramatic degradations of mechanical properties. Concerning the impact resistance, no rupture occurred using the 7.5 J pendulum as for the 3% red P composition, whereas the

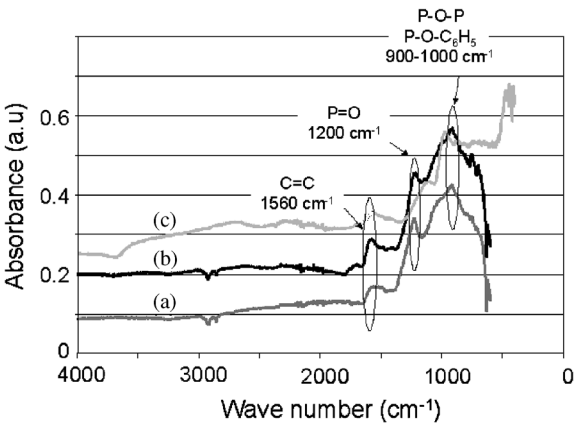

Figure 17. IRFT spectra of char of: (a) PET + 3% red P + 2% Fe_2O_3 at 500°C; (b) PET + 3% red P + 2% Fe_2O_3 at 600°C; and (c) PET + 3% red P at 500°C.

Table II. Mechanical properties of filled and unfilled PET.

Sample	Elongation at break (%)	Maximal tensile strength (MPa)	Impact resistance (kJ/m^2)
PET	>150	58.5	NR
3% red P	>150	55	NR
5% red P	>150	54	92.6
3% red P + 2% MgO	2	44	9.5
3% red P + 2% Fe_2O_3	>150	56	NR

NR: No rupture.

specimens broke for the 5% red P composition. A high value of elongation at break was obtained, showing the ductile character of the material. Moreover, the maximal tensile stress remained unchanged in comparison with the compositions containing only red P.

2.5. Use of additional reinforcements to improve the resistance of the char layer

Despite the improvements in fire performance due to the combination between red P and Fe_2O_3, the behaviour of the material in fire tests (particularly in epiradiateur test) seems not completely satisfactory due to a flowing of the molten polymer (Figure 18), including the charred upper layer. It is expected that a reinforcement of this layer could stop this flow, allowing a better protection of the material to be obtained. It was also shown that a viscosity control of flame-retarded thermoplastics at molten state could promote intumescence phenomena [10,11]. With this aim in view, talc and glass fibre were used as additive mineral reinforcements. Preliminary tests were performed using several percentages of glass fibre and talc in combination with 3% red P alone. A slight increase in LOI values was observed in both cases until a value of 6% for the reinforcing additive. From this value, LOI decreased due to a possible 'wick effect' related to the high thermal conductivity of the glass fibres in comparison with that of the polymer. In consequence, the following compositions were selected to carry out fire tests and mechanical characterizations:

- 3% red P + 6% glass fibres (GF)
- 3% red P + 6% talc
- 3% red P + 2% Fe_2O_3 + 6% glass fibres (GF)
- 3% red P + 2% Fe_2O_3 + 6% talc

The LOI values of the above compositions are compared with those of reference ones containing 3% red P + 2% Fe_2O_3 and only 3% red P (Figure 19). The presence of glass fibres

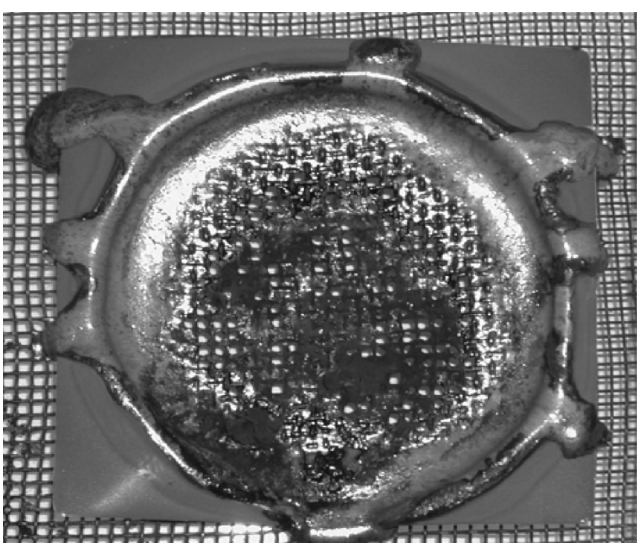

Figure 18. Optical micrograph showing the flowing of the molten polymer during the epiradiateur test.

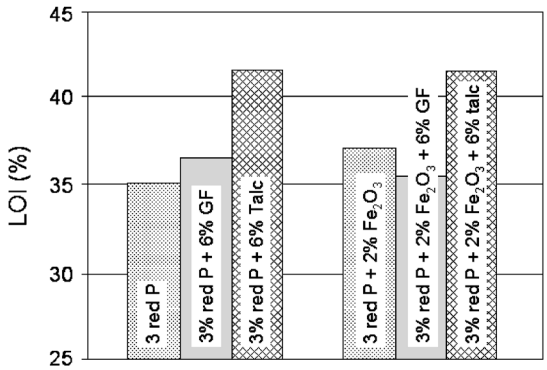

Figure 19. Limiting oxygen index (LOI) of PET compositions containing red P, Fe_2O_3, glass fibers (GF) or talc.

Table III. Epiradiateur test results of reinforced PET.

Sample	Ignition time (s)	Number of ignition	Mean inflammation period (s)	Maximal ignition period
3% red P	126	5.25	18	40
3% red P + 2% Fe_2O_3	119	14	7	9
3% red P + 6% GF	86	13	7.8	10
3% red P + 6% talc	74	15.4	10	20
3% red P + 2% Fe_2O_3 + 6% GF	85.5	8.4	6.6	9.5
3% red P + 2% Fe_2O_3 + 6% talc	60	24	7.5	13.5

tends to counterbalance the positive influence of iron oxide on LOI values. This can also be ascribed to the wick effect along the fibres which enhances the flame propagation. A reverse effect is noticed when talc is used, since LOI values higher than 36% are attained. This can be ascribed to the ability for the high specific surface area talc used (11 m^2/g) to build a protective layer after partial ablation of the polymer at the surface due to the combustion phenomenon. From the TGA curves performed in air, an improvement of the stability of residues is noticed when glass fibres and particularly talc are added to both iron oxide and red P: at 500°C, for the composition 3% red P + 2% Fe_2O_3 + 6% talc, the char residue corresponds to 34.7% of the initial weight and for the composition 3% red P + 2% Fe_2O_3, it represents only 23.3%.

This better stability is confirmed by the behaviour observed in epiradiateur tests, since a thin but expanded and very cohesive char layer is formed. Table III presents the epiradiateur test results. Ignition times are considerably reduced by the introduction of reinforcements. This can be explained by the increase in the thermal conductivity of the material, leading to a faster release of volatile combustible compounds which causes a rapid ignition. This effect can also be noticed on HRR curves (Figure 20) since the strong increase observed after ignition occurs at lower time values for the compositions containing glass fibres or talc. Despite epiradiateur test data did not indicate improvements concerning the ability to auto-extinguish, a decrease in peaks of HRR is noticed in Figure 20 (values lower than 150 kW/m^2 are obtained for the

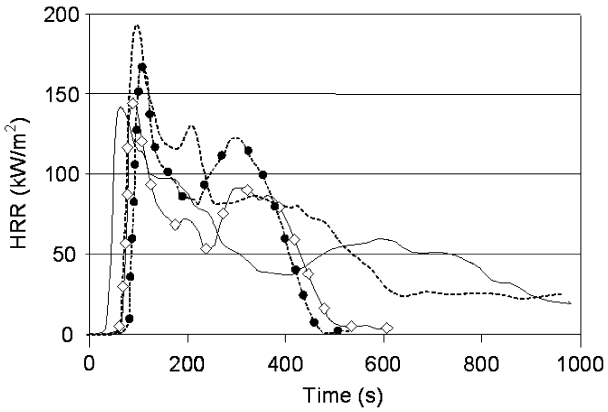

Figure 20. Heat release rate of filled PET as a function of time. (—) 3% red P + 6% GF, (- - -) 3% red P + 6% talc, (◇) 3% red P + 2% Fe_2O_3 + 6% talc, (●) 3% red P + 2% Fe_2O_3 + 6% GF.

Table IV. Mechanical properties of reinforced PET.

Sample	Elongation at break (%)	Maximal tensile strength (MPa)	Impact resistance (kJ/m^2)
3% red P + 6% GF	5	71.5	30
3% red P + 6% talc	5	54	39
3% red P + 2% Fe_2O_3 + 6% GF	5	70	20.5
3% red P + 2% Fe_2O_3 + 6% talc	4.7	58.5	32

compositions containing three components in PET). This can be ascribed to the formation of the expanded and charred layer, which improves the protection of the PET from the heat flux.

Finally, the influence of the incorporation of these reinforcements on the mechanical properties of the flame retarded PET was investigated. Table IV indicates the corresponding values and shows that PET has become more brittle due to the introduction of glass fibres or talc. Impact resistance and elongation at break are strongly reduced, while maximal tensile stress is at the same order than unfilled recycled PET.

3. CONCLUSION

The effectiveness of red phosphorus as flame retardant in PET is restricted to low percentages to avoid unfavourable effects on heat release after ignition. The use of mineral oxides such as MgO and Fe_2O_3 in combination with red phosphorus leads to synergistic effects on fire performance. Limiting oxygen index, ability to auto-extinguish, rate of heat release are improved when these oxides are used in substitution with red phosphorus. In addition, the char residue resulting from the combustion appears more stable in the case of these compositions. However, the mechanisms of action of MgO and Fe_2O_3 are not similar. While MgO can create a three-dimensional network by interacting with the acidic functions of PET chains, Fe_2O_3 is transformed into Fe_3O_4 and FeO and promotes the oxidation of red phosphorus to obtain

chemical structures present in the char layer formed after partial combustion of PET. It was also shown that in case of the use of MgO, its reactivity towards PET causes a collapse of mechanical properties, which can be ascribed to PET hydrolysis processes. To improve the mechanical stability of the char layer formed, small percentages of talc or glass fibres were added to the filled PET containing red phosphorus and iron oxide. They reduce heat release rate and improve thermal stability of the char layer, nevertheless PET losses its ductile character and exhibits impact resistance values which can restrict uses as engineering material.

REFERENCES

1. Muller AJ, Feijoo JL, Alvarez ME, Febles AC. The calorimetric and mechanical properties of virgin and recycled poly(ethylene terephthalate) from beverage bottles. *Polymer Engineering and Science* 1987; **27**:796.
2. Laoutid F, Ferry L, Lopez Cuesta JM, Crespy A. Red phosphorus/aluminium oxide compositions as flame retardants in recycled poly(ethylene terephthalate). *Polymer Degradation and Stability* 2003; **82**:357.
3. Yeh JT, Hsieh SH, Cheng YC, Yang MJ, Chen KN. Combustion and smoke emission properties of poly(ethylene terephthalate) filled with phosphorous and metallic oxides. *Polymer Degradation and Stability* 1998; **61**:399.
4. Levchik GF, Vorobyova SA, Gorbarenko VV, Levchik SV, Weil ED. Some mechanistic aspects of the fire retardant action of red phosphorus in aliphatic nylons. *Journal of Fire Science* 2000; **18**(3):172.
5. Weil ED. Oral communication. *2nd MoDeSt Conference*, Budapest, July 2002.
6. Weil ED, Patel NG. Iron compounds in non-halogen flame-retardant polyamide systems. *Polymer Degradation and Stability* 2003; **82**:291.
7. Laachachi A, Cochez M, Ferriol M, Lopez-Cuesta JM, Leroy E. Influence of TiO_2 and Fe_2O_3 fillers on the thermal properties of poly(methyl methacrylate) (PMMA). *Materials Letters* 2005; **59**:36.
8. Granzow A, Cannelongo JF. The effect of red phosphorus on the flammability of poly(ethylene terephthalate). *Journal of Applied Polymer Science* 1976; **20**:689.
9. Granzow A, Ferrillo RG, Wilson A. The effect of elemental red phosphorus on the thermal degradation of poly(ethylene terephthalate). *Journal of Applied Polymer Science* 1977; **21**:1687.
10. Lopez Cuesta JM, Durin A, Ferry L, Leroy E. Improvement of fire behaviour of EVA using binary and ternary mineral compositions. *14th International BCC-Conference Flame Retardancy of Polymeric Materials*, Stamford, CT, U.S.A., June 2003.
11. Ferry L, Gaudon P, Leroy E, Lopez-Cuesta JM. In *Fire Retardancy of Polymers*: *The Use of Mineral Fillers*, Le Bras M, Wilkie C, Bourbigot S, Duquesne S, Jama C (eds). Royal Society of Chemistry: Oxford, 2004; 345.